TÜBİTAK

Turkish Journal of Physics

http://journals.tubitak.gov.tr/physics/

Research Article

Turk J Phys
(2022) 46: 104 – 112

doi:10.3906/fiz-2111-1

The fine spectral tuning of plasmon mode and quantum emitter coupling and its comparison with the dark-hot resonances

Hira ASIF[1], **Rasim Volga OVALI**[2], **Ramazan ŞAHİN**[1*]
[1]Department of Physics, Akdeniz University, Antalya, Turkey
[2]Department of Physics, Recep Tayyip Erdoğan University, Rize, Turkey

Received: 03.11.2021 • **Accepted/Published Online:** 16.03.2022 • **Final Version:** 28.04.2022

Abstract: Localization of incident fields into very small volumes (hot-spots) allows strong light-matter interactions at the hot spots. This makes path interference effects, Fano resonances, visible. Fano resonances can appear due to the coupling of a bright plasmon (i) to a longer lifetime dark plasmon mode or (ii) to a quantum object (QO) of a much longer lifetime. The second phenomenon provides a very important utility: the voltage tunability of the linear/nonlinear response. The level-spacing of the QO, such as defect-centers and quantum dots, are voltage-tunable which can make a sharp Fano resonance appear and disappear. Here, we compare the two phenomena by solving the equations of motions for the near-field plasmon amplitudes, derived from two different Hamiltonians. While the two plasmon amplitudes look similar to each other, except for the population inversion parameter 'y', our results show that quantum emitter enables fine spectral tuning of the plasmon amplitude, thus, providing better enhancement.

Keywords: Localized surface plasmon (LSP), long-lived oscillators, bright and dark plasmon modes, fine-tuning response

1. Introduction

Plasmonics is a pioneering field of photonics [1, 2] in which the quantization of collective oscillations of free electrons in metals is defined as plasmons [3, 4]. These plasmons can be localized by confining around the nanoparticles (also known as localized surface plasmon-LSP) [5] or they can propagate (as surface plasmon polaritons-SPP) along the metal-dielectric interface [6] in periodic nanostructures. Since both localized and propagating modes of surface plasmons are sensitive to their environmental conditions, they can be used for a variety of applications ranging from single-molecule detection to increasing solar-cell efficiency [7–9]. In this field, the main motivation is therefore not only exploring the light-matter interaction at the nanoscale dimensions but also to control the field localization and enhancement of incident electromagnetic field for a variety of applications [10–12] through surface plasmon resonance (SPR). In addition, huge progress in lithographic techniques [13], direct laser ablation [14, 15], and wet-chemical processes [16] give the possibility of precisely adjusting the size, the shape, and the periodicity of plasmonic structures to tune the spectral position of SPR in the visible region of electromagnetic spectrum [17]. These plasmonic structures can be utilized as a platform for

*Correspondence: rsahin@itu.edu.tr

active tuning of SPR spectral position with single-layer graphene (SLG) [18]. Moreover, the localized field in the coupled plasmonic system can be used to enhance nonlinear processes such as Raman signals[19]. Unlike all above applications of plasmonic phenomenon, strong localization of incident field into very small hot-spots enables new research areas to be opened, known as *quantum optics* [20] and *quantum plasmonics* [21, 22]. In general, tiny objects such as quantum dot (QD), quantum emitter (QE) [23–25] or nowadays defect/color centers [26, 27] are positioned very close to plasmonic nanostructures to acquire very interesting physical phenomena such as *Fano resonances (FRs)* or *path interference effect*. Since these are the plasmon analogs of electromagnetically induced transparency (EIT) [28–30], a deep understanding of the physics behind EIT is crucial. In EIT, the excited state is weakly hybridized into two, by the interaction of a strong microwave pump source, where these two states operate out of phase so one absorbs the incident energy as the other one emits. However, the strong microwave pump source induces weak hybridization of the excited level as opposed to FRs [31]. FRs or path interference can possess strong potential to control both plasmon amplitude and lifetime of plasmon oscillations in linear and nonlinear regimes [32–39]. Although FRs or sometimes referred as path interference effects possess quantum mechanical nature, they are experimentally observed in which long-lifetime plasmon mode (dark mode) interacts with the bright plasmon mode [34].

Advancements in technology and the progression in the micro and nano-fabrication facilities allow us to produce complex nanostructures for plasmonic applications to support dark modes. However, dark plasmon modes (antibonding plasmon mode or quadrupole mode) cannot be directly excited with linearly polarized light sources. On the other hand, this effect can also be accomplished by quantum objects (QE, QD or molecules) where the interaction appearing between bright-dark plasmon coupling owns the same nature as the interaction between bright plasmon mode and QE [40] except for a population inversion parameter. We present here a very detailed explanation to clarify this difference for plasmonic applications as follows. First, we obtain the plasmon amplitudes for these two different scenarios with steady-state solutions of Heisenberg equations. Then, we explain the fine-tuning of plasmon amplitudes with dark modes due to missing population inversion parameter in bright-dark plasmon coupled system before the conclusion.

2. Theoretical model

In this section, the bright-dark plasmons coupling is first explained on the model system through a quantum mechanical approximation. For this purpose, we assume that a single spherical Au nanoparticle (AuNP) is positioned very close to Ag metal nanorod (AgNR) dimer (Figure 1 (a)). Here, Au nanoparticle supports localized plasmon modes (bright mode) while metal nanorod dimer supports dark-mode provided that the polarization of illuminating source becomes along with the distance between nanorods. In our analytical model, we assume these modes as interacting/coupled harmonic oscillators. We start with writing the total energy of the system in the Heisenberg picture to reach the plasmon amplitude of coupled system as follows.

$$\hat{H}_0 = \hbar\Omega_b \hat{a}_b^\dagger \hat{a}_b + \hbar\Omega_d \hat{a}_d^\dagger \hat{a}_d, \tag{1}$$

$$\hat{H}_P = i\hbar(\varepsilon \hat{a}^\dagger e^{-i\omega t} - \text{h.c}), \tag{2}$$

$$\hat{H}_{int} = \hbar f(\hat{a}_b^\dagger \hat{a}_d + \hat{a}_d^\dagger \hat{a}_b). \tag{3}$$

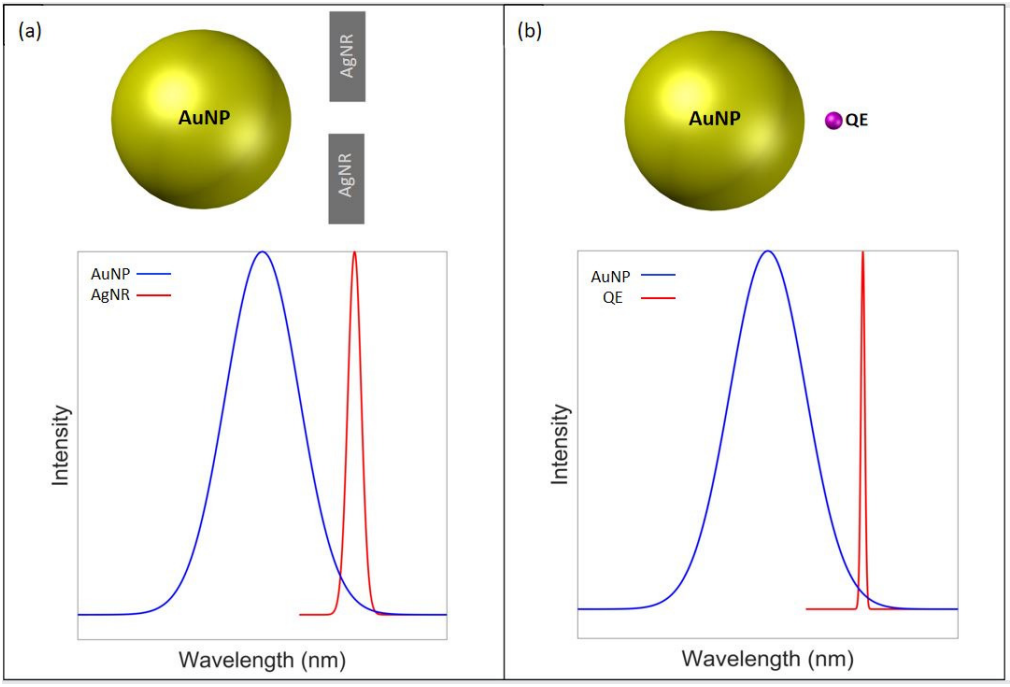

Figure 1. (a) Au nanoparticle (AuNP) supporting bright plasmon mode and Ag nanorod (AgNR) supporting dark plasmon mode in a coupled plasmonic system with individual responses as a function of wavelength. (b) AuNP and Quantum emitter (QE) in the coupled systems and their corresponding response functions.

Here, $\hat{H}_0$ includes energies of bright ($\hbar\Omega_b\hat{a}_b^\dagger\hat{a}_b$) and dark plasmon ($\hbar\Omega_d\hat{a}_d^\dagger\hat{a}_d$) modes, respectively, where $\hat{a}^\dagger$ ($\hat{a}$) is creation (annihiliation) operator. In addition, Ω_b and Ω_d are the resonance frequencies of the oscillators. The coupling between bright-dark mode is included as $\hat{H}_{int}$ in which f is a measure of this coupling in unit of energy (interaction strength). Finally, $\hat{H}_P$ is the energy of pump source (ω is the excitation frequency). The equations of the motion can be obtained by applying Heisenberg equation, $i\hbar\dot{\hat{a}} = [\hat{a}, \hat{H}]$. Since amplitudes (number of plasmons to be excited) define plasmon excitation, the operators $\hat{a}_b$ and $\hat{a}_d$ are replaced with complex numbers α_b and α_d, respectively [41].

$$\dot{\alpha_b} = -(i\Omega_b + \gamma_b)\alpha_b - if\alpha_d + \varepsilon e^{-i\omega t} \tag{4a}$$

$$\dot{\alpha_d} = -(i\Omega_d + \gamma_d)\alpha_d - if\alpha_b \tag{4b}$$

γ_b and γ_d are the decay rates of the plasmon fields. In the steady-state, both oscillators follow the driving frequency of ω so the final plasmon amplitude of coupled system can be obtained as in Equation 5.

$$\tilde{\alpha_b} = \frac{\varepsilon}{[i(\Omega_b - \omega) + \gamma_b] + \frac{|f|^2}{[i(\Omega_d - \omega) + \gamma_d]}}, \tag{5}$$

To analyze the spectral response of bright plasmon mode upon coupling to the dark mode we plot the plasmon mode intensity as a function of excitation frequency ω as shown in Figure 2. We point

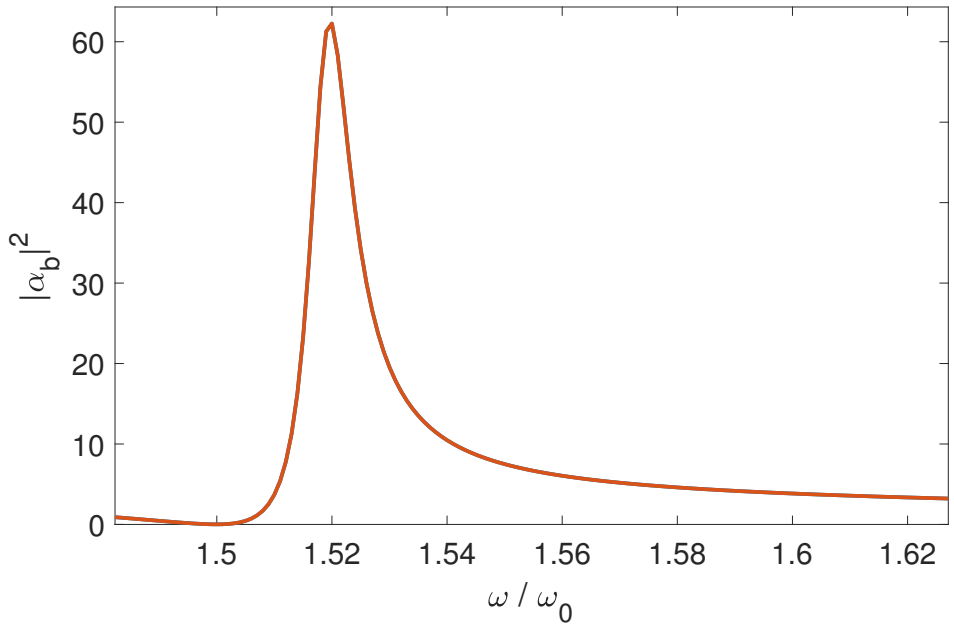

Figure 2. Intensity of bright plasmon mode plotted as a function of normalized excitation frequency ω/ω_0 when dark mode coupled to bright plasmon mode, obtained from Equation 5 with parameters taken as $\Omega_b = 1.0\omega_0$, $\Omega_d = 1.5\omega_0$, $\gamma_b = 0.1\omega_0$, $f = 0.1\omega_0$ and $\gamma_d = 0.001\omega_0$.

out here that dark-plasmon mode serves as a longer lifetime oscillator. Therefore, we can replace dark-plasmon mode with QE/QD systems because they possess smaller decay rate values than bright plasmon fields ($\gamma_b > \gamma_{eg}$). Figure 1 (b) shows the model system consisting of Au nanoparticle and QE. One can write the total Hamiltonian system and calculate the plasmon field of coupled oscillators as explained above. The Hamiltonian of the coupled system (Figure 1 (b)) is written as the sum of the energy of the plasmon oscillation (Ω_b), quantum emitter ($\omega_{\rm eg}$), the pump source (ω), and the interaction between QE and plasmon field ($\hat{H}_{int}$) as follows.

$$\hat{H}_0 = \hbar\Omega_b\hat{a}_b^\dagger\hat{a}_b + \hbar\omega_{eg}|e\rangle\langle e|, \tag{6}$$

$$\hat{H}_P = i\hbar(\varepsilon\hat{a}_b^\dagger e^{-i\omega t} - \text{h.c}), \tag{7}$$

$$\hat{H}_{int} = \hbar f(\hat{a}_b^\dagger|g\rangle\langle e| + \hat{a}_b|e\rangle\langle g|). \tag{8}$$

Here $|g\rangle$ ($|e\rangle$) is the ground (excited) state of the QE. $\gamma_b, \gamma_{\rm eg}$, and $\gamma_{\rm ee}$ are the decay rates of plasmon mode, off-diagonal and diagonal elements of QE's density matrix, respectively, which yield the following equations for the amplitudes.

$$\dot{\alpha_b} = -(i\Omega_b + \gamma_b)\alpha_b - if\rho_{ge} + \varepsilon e^{-i\omega t} \tag{9a}$$

$$\dot{\rho}_{ge} = -(i\omega_{\rm eg} + \gamma_{eg})\rho_{ge} + if\alpha(\rho_{ee} - \rho_{gg}) \tag{9b}$$

$$\dot{\rho}_{ee} = -\gamma_{ee}\rho_{ee} + i(f\rho_{ge}\alpha^* - c.c) \tag{9c}$$

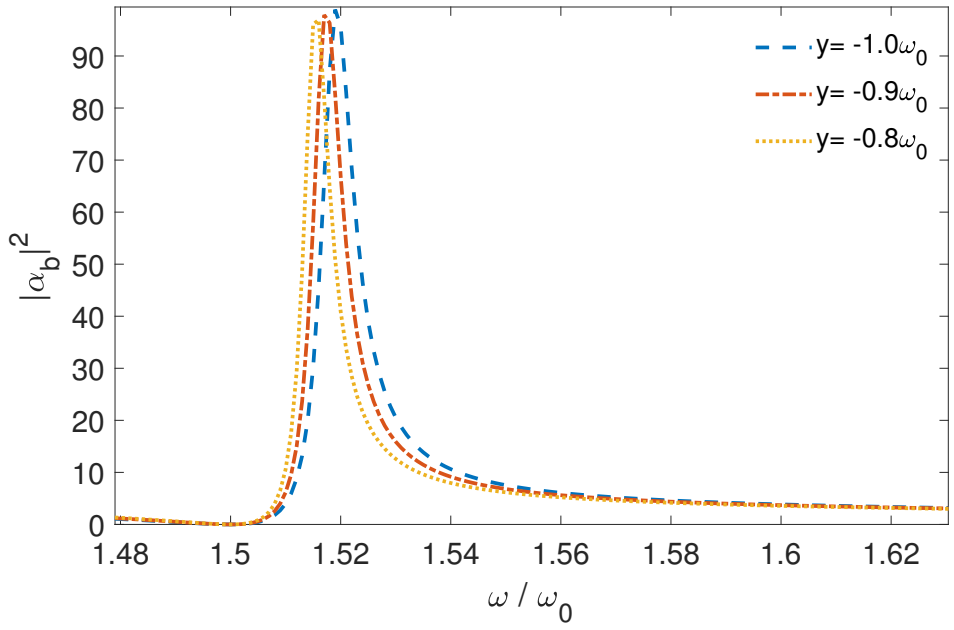

Figure 3. Intensity of bright plasmon mode plotted as a function of normalized excitation frequency ω/ω_0 when QE coupled to bright plasmon mode, obtained from Equation10 for different values of population inversion parameter y, while other parameters are taken as $\Omega_b = 1.0\omega_0$, $\omega_{\rm eg} = 1.5\omega_0$, $\gamma_b = 0.1\omega_0$, $f = 0.1\omega_0$, and $\gamma_{eg} = 10^{-6}\omega_0$.

In the steady state, oscillations of the plasmon amplitude ($\alpha_b = \tilde{\alpha_b}e^{-i\omega t}$) and off-diagonal density matrix element ($\rho_{ge} = \tilde{\rho}_{ge}e^{-i\omega_{\rm exc}t}$) result in Equation 10, where $y = \rho_{ee} - \rho_{gg}$ is the population inversion parameter.

$$\tilde{\alpha_b} = \frac{\varepsilon}{[i(\Omega_b - \omega) + \gamma] - \frac{|f|^2 y}{[i(\omega_{\rm eg} - \omega) + \gamma_{\rm eg}]}} \tag{10}$$

Here, one must take into account the conservation of probability, $\rho_{ee} + \rho_{gg} = 1$ and we assume that the diagonal density matrix element does not oscillate in the steady-state ($\rho_{ii} = \tilde{\rho}_{ii}$ (i=e, g)). One can easily notice that Equation 5 and Equation 10 exactly resemble each other except for the population inversion parameter 'y'. Both equations cause the plasmon amplitude of a damped cavity if the interaction term is absent ($f = 0$). Moreover, the response of the system is weak when $\omega_{\rm exc}$ and $\Omega_{\rm b}$ are not close to each other (off-resonant excitation scheme). On the other hand, the denominators of Equation 5 and Eq. 10 clearly indicate the role of interaction between two-oscillators on the tuning of resulted plasmon amplitude with f, Ω_d ($\omega_{\rm eg}$), and $\gamma_{\rm d}$ ($\gamma_{\rm eg}$) parameters.

Coupling between two oscillators ($f \neq 0$) yields minimization of the denominators in Equation 5 and Equation 10 with an appropriate Ω_d ($\omega_{\rm eg}$) value to enhance the plasmon amplitude ($\tilde{\alpha}$). In practice, this can be done by placing an auxiliary molecule (a variety of molecules can be found for this purpose in [42]) in close proximity of plasmonic system or designing (size, shape, or material type) an appropriate metal nanorod dimer to support dark plasmon mode. Although all these are widely discussed in the literature and yield more fine control of linear and nonlinear plasmon amplitudes,

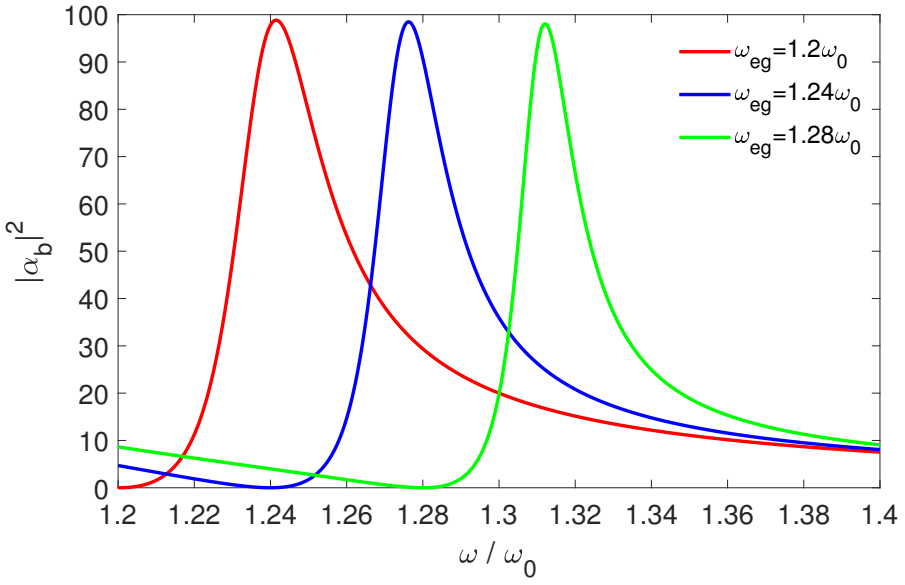

Figure 4. Intensity of bright plasmon mode calculated for different frequencies of QE using Equation 10 while other parameters are $\Omega_b = 1.0\omega_0$, $\gamma_b = 0.1\omega_0$, $\gamma_{eg} = 10^{-6}\omega_0$, and $f = 0.1\omega_0$.

the importance of the population inversion parameter, 'y' (see the second term in the denominator of Equation 10) is not certainly noticed yet. Though, without 'y' parameter, the coupled system is exactly solvable. But, the addition of 'y' requires time-evolution to determine its value even in the steady-state for which the parameter 'y' takes a negative value (between –1 and 0). Moreover, the response function of Equation 10 in the presence of 'y' becomes always higher than that of Equation5 which makes it a more flexible controlling scheme than a bright-dark plasmon coupled system. To investigate the role of y parameter in the coherent response of coupled plasmon system we calculate the intensity of bright plasmon mode for different values of y as shown in Figure 3. The result obtained from Equation 10 (see Figure 3) shows a clear distinction from Figure 2 in terms of the peak intensity of the bright plasmon mode. This is due to the 'y parameter' provided by QE in the denominator of steady-state amplitude Equation 10 which escalates the peak intensity of bright plasmon mode in the coupled state. In other words, one can reach higher plasmon amplitudes in bright-QE plasmon coupling when it is compared to bright-dark plasmon coupling system even Equation 5 and Equation 10 are quite similar. Recent studies indicate that stress-induced defect centers can be used as quantum emitters/quantum objects. Moreover, the operation wavelength in which we refer to this as level spacing in our theoretical model for quantum emitter can be adjusted with an external voltage. Therefore, controlling defect resonance provides an additional tuning capability of the Fano response of the coupled plasmonic system. Next, we explore the fine spectral tuning of the quantum emitter with the bright plasmon mode under weak coupling for different level spacing ω_{eg} as shown in Figure 4. The sharp resonance of quantum emitter provided by discrete level spacing is electrically tunable which supports coherent quantum states in defect centers and quantum dots [43, 44]. The tunable spectral response of these systems make them more propitious over dark hot resonances to control and probe the plasmonic systems for ultrahigh-resolution single-molecule imaging [27] and pave its way for silent enhancement of plasmon amplitude in the surface-enhanced Raman spectroscopy SERS [33].

3. Conclusion

We explore theoretically the differences between bright-dark plasmon coupling and bright plasmon-QE coupling even though they seem very similar. First, we clarify the plasmon amplitudes obtained from the total Hamiltonian of the model systems in the Heisenberg picture. Then, we analyze the tuning of resulted plasmon field with respect to the properties of coupled oscillators. The results of this comparison and analysis show that the bright plasmon-QE coupled system exhibit enhanced plasmon field amplitude ($\tilde{\alpha}$), due to the 'y-population' parameter as compared to the bright-dark plasmon coupled system. In addition to this, QE provides a more flexible fine spectral tuning by coupling to the bright plasmon resonant mode. Finally, we conclude that the voltage tunable property of stress-induced defect centers which can serve as quantum emitters enables spectral tuning of Fano response of plasmon-defect center coupling.

Acknowledgement

R.S. acknowledges support from TUBITAK - Project No. 121F030.

References

[1] E. Ozbay, "Plasmonics: merging photonics and electronics at nanoscale dimensions," *Science* **311** (2006) 189.

[2] S. A. Maier, "Plasmonics: Fundamentals and Applications," Springer, New York, USA, (2007).

[3] E. Kretschmann, H. Raether, "Radiative Decay of Non Radiative Surface Plasmons Excited by Light," *Zeitschrift für Naturforschung A* **23** (2014) 2135.

[4] A. Otto, "Excitation of nonradiative surface plasma waves in silver by the method of frustrated total reflection," *Zeitschrift fur Physik A Hadrons and nuclei* **216** (1968) 398.

[5] K. L. Kelly, E. Coronado, L. L. Zhao, G. C. Schatz, "The Optical Properties of Metal Nanoparticles: The Influence of Size, Shape, and Dielectric Environment," *The Journal of Physical Chemistry B* **107** (2003) 668.

[6] S. Zeng, D. Baillargeat, H. P. Ho, K.T. Yong, "Nanomaterials enhanced surface plasmon resonance for biological and chemical sensing applications," *Chem. Soc. Rev.* **43** (2014) 3426.

[7] D. K. Lim, K.S. Jeon, H. M. Kim, J. M. Nam, Y. D. Suh, "Nanogap-engineerable Raman-active nanodumbbells for single-molecule detection," *Nature Materials* **9** (2010) 60.

[8] N.J. Halas, S. Lal, W. S. Chang, S. Link, P. Nordlander, "Plasmons in Strongly Coupled Metallic Nanostructures," *Chemical Reviews* **111** (2011) 3913.

[9] F. Enrichi, A. Quandt, G. C. Righini, "Plasmonic enhanced solar cells: Summary of possible strategies and recent results," *Renewable and Sustainable Energy Reviews* **82** (2018) 2433.

[10] T. Chung, S. Y. Lee, E. Y. Song, H. Chun, B. Lee, "Plasmonic Nanostructures for Nano-Scale Bio-Sensing," *Sensors* **11** (2011) 10907.

[11] W. Zhang, L. Huang, C. Santschi, O. J. F. Martin, "Trapping and Sensing 10 nm Metal Nanoparticles Using Plasmonic Dipole Antennas," *Nano Letters* **10** (2010) 1006.

[12] A. V. Kabashin, P. Evans, S. Pastkovsky, W. Hendren, G. A. Wurtz et al., "Plasmonic nanorod metamaterials for biosensing," *Nature Materials* **8** (2009) 867.

[13] F. Hong, R. Blaikie, "Plasmonic Lithography: Recent Progress," *Advanced Optical Materials* **7** (2019) 1801653.

[14] R. Sahin, Y. Morova, E. Simsek, S. Akturk, "Bessel-beam-written nanoslit arrays and characterization of their optical response," *Applied Physics Letters* **102** (2013) 193106.

[15] E. Simsek, S. Akturk, "Plasmonic Enhancement During Femtosecond Laser Drilling of Sub-wavelength Holes in Metals," *Plasmonics* **6** (2011) 767.

[16] X. Lu, M. Rycenga, S. E. Skrabalak, B. Wiley, Y. Xia, "Chemical Synthesis of Novel Plasmonic Nanoparticles," *Annual Review of Physical Chemistry* **60** (2009) 167.

[17] H. Ditlbacher, A. Hohenau, D. Wagner, U. Kreibig, M. Rogers et al., "Silver Nanowires as Surface Plasmon Resonators," *Phys. Rev. Lett.* **95** (2005) 257403.

[18] E. Simsek, "Improving Tuning Range and Sensitivity of Localized SPR Sensors With Graphene," *IEEE Photonics Technology Letters* **25** (2013) 867.

[19] D. Cialla, A. Marz, R. Bohme, F. Theil, K. Weber et al., "Surface-enhanced Raman spectroscopy (SERS): progress and trends," *Analytical and Bioanalytical Chemistry* **403** (2012) 27.

[20] I. A. Walmsley, "Quantum optics: Science and technology in a new light," *Science* **348** (2015) 525.

[21] M. S. Tame, K. R. McEnery, K. Ozdemir, J. Lee, S. A. Maier et al., "Quantum plasmonics," *Nature Physics* **9** (2013) 329 .

[22] J. I. Cirac, H. J. Kimble, "Quantum optics, what next?," *Nature Photonics* **11** (2017) 18.

[23] A. Manjavacas, F.J. García de Abajo, P. Nordlander, "Quantum Plexcitonics: Strongly Interacting Plasmons and Excitons," *Nano letters* **11** (2011) 2318.

[24] K. Santhosh, O. Bitton, L. Chuntonov, G. Haran, "Vacuum Rabi splitting in a plasmonic cavity at the single quantum emitter limit," *Nature Communications* **7** (2016) ncomms11823.

[25] A. Delga, J. Feist, J. Bravo-Abad, F. J. Garcia-Vidal, "Theory of strong coupling between quantum emitters and localized surface plasmons," *Journal of Optics* **16** (2014) 114018.

[26] S. Kumar, A. Huck, U. L. Andersen, "Efficient Coupling of a Single Diamond Color Center to Propagating Plasmonic Gap Modes," *Nano Letters* **13** (2013) 1221.

[27] R. V. Ovali, R. Sahin, A. Bek, M. E. Tasgin, "Single-molecule-resolution ultrafast near-field optical microscopy via plasmon lifetime extension," *Applied Physics Letters* **118** (2021) 241103.

[28] S.E. Harris, "Electromagnetically Induced Transparency," *Physics Today* **50** (1997) 36.

[29] M. O. Scully, M. S. Zubairy "Quantum Optics," Cambridge Univ. Press, U.K., (1997).

[30] M. O. Scully, M. S. Zubairy, "Quantum Optics," *American Journal of Physics* **67** (1999) 648.

[31] M. Tasgin, A. Bek, S. Postaci, "Fano Resonances in the Linear and Nonlinear Plasmonic Response," In Book: Fano Resonances in Optics and Microwaves: Physics and Application, Springer, Switzerland, (2018).

[32] S. K. Singh, M. K. Abak, M. E. Tasgin, "Enhancement of four-wave mixing via interference of multiple plasmonic conversion paths," *Physical Review B* **93** (2016) 035410.

[33] S. Postaci, B. C. Yildiz, A. Bek, M. E. Tasgin, "Silent enhancement of SERS signal without increasing hot spot intensities," *Nanophotonics* **7** (2018) 1687.

[34] B. C. Yildiz, A. Bek, M. E. Tasgin, "Plasmon lifetime enhancement in a bright-dark mode coupled system," *Physical Review B* **101** (2020) 035416.

[35] R. Sahin, "Control of EOT on sub-wavelength Au hole arrays via Fano resonances," *Optics Communications* **454** (2020) 124431.

[36] M. Gunay, V. Karanikolas, R. Sahin, R. V. Ovali, A. Bek et al., "Quantum emitter interacting with graphene coating in the strong-coupling regime," *Physical Review B* **101** (2020) 165412.

[37] Z. Artvin, M. Gunay, A. Bek, M. E. Tasgin, "Fano-control of down-conversion in a nonlinear crystal via plasmonic–quantum emitter hybrid structures," *Journal of the Optical Society of America B* **37** (2020) 3769.

[38] R. Sahin, "Improving field localization and figure-of-merit value in plasmonic structures via path-interference effect," *Superlattices and Microstructures* **133** (2019) 106218.

[39] M. Gunay, Z. Artvin, A. Bek, M. E. Tasgin, "Controlling steady-state second harmonic signal via linear and nonlinear Fano resonances," *Journal of Modern Optics* **67** (2020) 26.

[40] M. E. Tasgin, "Metal nanoparticle plasmons operating within a quantum lifetime," *Nanoscale* **5** (2013) 8616.

[41] M. Premaratne, M. I. Stockman, "Theory and technology of SPASERs," *Advances in Optics and Photonics* **9** (2017) 79.

[42] M. Taniguchi, J. S. Lindsey, "Database of Absorption and Fluorescence Spectra of >300 Common Compounds for use in PhotochemCAD," *Photochemistry and Photobiology* **94** (2018) 290.

[43] C. Chakraborty, L. Kinnischtzke, K. M. Goodfellow, R. Beams, A. N. Vamivakas, "Voltage-controlled quantum light from an atomically thin semiconductor," *Nature Nanotechnology* **6** (2015) 507-511.

[44] S. Schwarz, A. Kozikov, F. Withers, J. K. Maguire, A. I. Tartakovskii, "Electrically pumped single-defect light emitters in WSe_2," *2D Materials* **6** (2016) 025038.